HIGH-POWER BROADBAND AlGaN/GaN HEMT MMIC's ON SiC SUBSTRATES

Bruce M. Green[†], Vinayak Tilak[†], Sungjae Lee [*], Hyungtak Kim[†], Joseph A. Smart[†], Kevin J. Webb[*], James R. Shealy[†], and Lester F. Eastman[†]

Abstract— **Broadband, high power cascode AlGaN/GaN HEMT MMIC amplifiers with high gain and power-added efficiency (PAE) have been fabricated on high-thermal conductivity SiC substrates. A cascode gain cell exhibiting 5 W of power at 8 GHz with a small signal gain of 19 dB was realized. A broadband amplifier MMIC using these cascode cells in conjunction with a lossy-match input matching network was designed, fabricated, and evaluated, showing a useful operating range of DC-8 GHz with an output power of 5-7.5 W and a PAE of 20-33 % respectively. A nonuniform distributed amplifier (NDA) based on this same process yielded an output power of 3-6 W over a DC-8 GHz bandwidth with an associated PAE of 13-31 %.**

Keywords— **Cascode, GaN, Distributed Amplifier, Broadband Amplifier**

FOR decades, the realization of broadband, high power MMIC power amplifiers has posed a significant challenge to microwave design and systems engineers due to the electrical and thermal limitations of GaAs transistor technology. In recent years, AlGaN/GaN HEMT technology has established itself as a strong contender for such applications because of its large electron velocity ($> 1 \times 10^7$ cm/s), bandgap (3.4 eV), breakdown voltage (>50 V for f_T = 50 GHz), and sheet carrier concentration ($n_S > 1 \times 10^{13}$ cm^{-2}). Due to the superior electronic properties of the material and the possibility to grow the material on high thermal conductivity (3.5 W/cm-°K) SiC substrates, power densities as high as 9.2 W/mm at 8.2 GHz [1] and 4 W/mm at 16 GHz [2] have been achieved.

This paper addresses the problems associated with broadband, high-power MMIC power amplifiers on both the device technology and circuit design fronts by the use of high-performance AlGaN/GaN HEMT's in MMIC amplifier configurations optimized for high power and PAE. Previous work on GaN-based circuits has shown the viability of these devices for microwave circuit applications [3], [4], [5], [6]. However, to date no broadband power amplifier MMIC results have been achieved using high thermal conductivity SiC substrates. This paper describes the design and development of the first multi-octave broadband MMIC's based on AlGaN/GaN HEMT's fabricated on high thermal conductivity SiC substrates for simple, efficient device heat sinking. First, technology used to fabricate the active and passive devices on SiC substrates is described. Next, the large signal operation of the cascode power cell in terms of its dynamic loadline behavior is compared to the measured DC $I-V$ characteristics for the device, showing strong correlation of the DC and microwave current. Results for cascode pairs of 0.25 mm and 1 mm peripheries show excellent power scaling properties, as both devices realized output power densities of ≥ 5 W/mm (≥ 36 % PAE) at 8 GHz at a drain bias of 30 V. Finally, the design and characteristics of cascode broadband power MMIC's using both lossy-match and distributed amplifier designs are given. In each case, a DC-8 GHz bandwidth was achieved with output powers of 5-7.5 W and 3-6 W and associated PAE's of 20-33 % and 13-31 % respectfully.

[†]School of Electrical and Computer Engineering, Cornell University, Ithaca, NY 14853 E-mail: green@iiiv.tn.cornell.edu. [*]School of Electrical and Computer Engineering, Purdue University, W. Lafayette, IN 47907. This work is supported under ONR MURI Contract N00014-96-1-1223, monitored by Dr. John Zolper

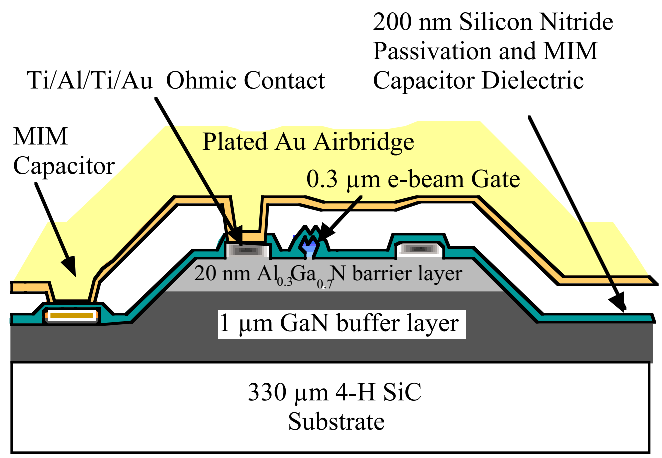

Fig. 1. Cross sectional diagram showing MMIC process for AlGaN/GaN HEMT's on SiC substrates.

I. Gallium Nitride HEMT MMIC Technology

A simple seven mask level MMIC process, as shown in Figure 1, was used to fabricate the devices and circuits of this work. The wafers used to fabricate the MMIC's are grown by organo-metallic vapor phase expitaxy and consist of a 50 nm AlGaN nucleation layer followed by a 1-1.5 μm GaN buffer and $Al_{0.3}Ga_{0.7}N$ barrier layers grown on 4-H SiC substrates. Alignment marks are formed with Pt for both e-beam and optical alignments. Next, mesas for active transistors as well as resistors are etched to a depth of 220 nm using a Cl_2-based electron-cyclotron resonance (ECR) etching tool. Ohmic contact to the two-dimensional electron gas is accomplished by the use of a Ti (20nm)/ Al (120 nm)/ Ti (45 nm)/Au (55 nm) ohmic contact metal stack that is patterned using an e-beam liftoff process and then annealed in an 800 °C N_2 ambient for 30 s. Mushroom gates are formed using direct e-beam writing in conjunction with a tri-level resist scheme. All devices have a gate length of 0.3 μm. The first level interconnect metal is patterned using optical lithography and the lift-off technique. A 200 nm Si_3N_4 passivation/dielectric layer is applied after the interconnect metal to passivate the high-field regions of the devices, as well as to form a dielectric for MIM capacitors. Past studies [7] indicate that this passivation layer plays a role in helping to suppress long time constant charge storage in surface states in the high field surface region of our undoped HEMT devices. Following the passivation step, holes are etched in the Si_3N_4 using reactive ion etching to allow for contact to the first level interconnect metal. Airbridges are then plated to a thickness of 2.5 μm using a two level optical resist and electroplating scheme.

II. Dynamic Loadline and Power Scaling of Cascode-Connected Gallium Nitride HEMT's

The circuits presented here use the cascode configuration due to the high gain associated with its low feedback capacitance and output conductance. In this relatively immature AlGaN/GaN HEMT transistor technology, electron trapping effects have been known to cause the microwave channel current and hence output power to be lower than that predicted by DC $I-V$ curves [7]. Figure 2 compares the measured 8 GHz dynamic loadline behavior of two cascode-connected 0.3×250 μm^2 devices to their measured DC $I-V$ characteristics. The figure shows good correlation between the DC $I-V$ curves and the realized microwave current and voltage swings. The dynamic loadline measurement was performed using a 4-26.5 GHz Maury™ load-pull system with HP 708208A microwave transition analyzers (MTA's) used in place of power meters [8]. Because of the large bandgap and hence the large breakdown voltage and maximum channel current evidenced by the dynamic loadline, a high power density of 4.5 W/mm was obtained under the bias conditions of $V_D = 25$ V, $V_{G1} = -3$ V, and $V_{G2} = +5$ V.

Figure 3 demonstrates the excellent power scaling properties of the cascode pair due, in part, to the high thermal conductivity SiC substrate. The figure compares the output power density, gain, and PAE of the $W_1 = W_2 = 0.250$ mm device with that of a $W_1 = W_2 = 1$ mm device. In each case, a power density of 5 W/mm and a PAE of 36 % was met or exceeded at a bias point of $V_D = 30$ V, $V_{G1} = -3$ V, and $V_{G2} = +5$ V.

III. Design and Characteristics of High-Power Broadband MMIC's

The MMIC's presented here will be used as high-efficiency power cells for push-pull operation. To this end, they are designed for characteristic impedances of 25 Ω on the input and output. The design of these broadband MMIC's offers significant advantages over conventional distributed amplifiers for efficient large signal operation. Distributed amplifiers (DAs) offer broadband operation by incorporating gain elements in synthetic, lumped-element approximate transmission lines, realized by the transistor capacitances and intervening inductances [9]. However, conventional DAs do not have good PAE because (1) power is consumed by the synthetic drain line termination dummy load, (2) the devices are loaded nonuniformly along the drain line, and (3) frequency-dependent attenuation along the gate line results in nonuniform drive of the active devices. The design of a lossy-match cascode power amplifier and a nonuniform distributed power amplifier discussed below address the power and PAE deficiencies of the conventional DA approach.

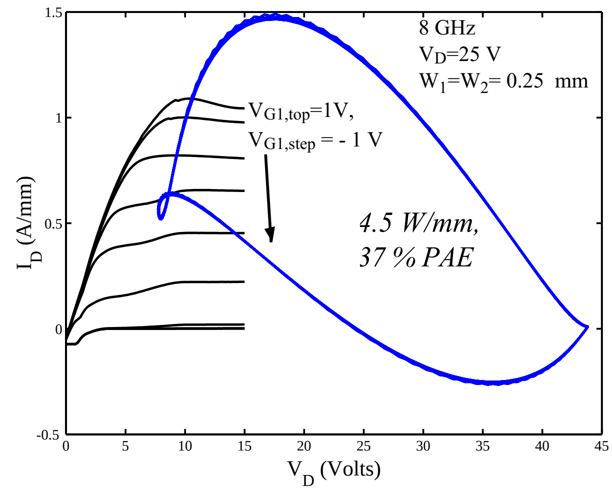

Fig. 2. 8 GHz dynamic loadline and DC $I-V$ curves ($V_{G1,top} = +1$ V, $V_{G1,step} = -1$ V) for cascode cell with $W_1 = W2 = 250$ μm and $L_{G1,G2} = 0.3$ μ m. Bias: $V_D = 25$V, $V_{G1} = -3$ V, $V_{G2} = +5$ V.

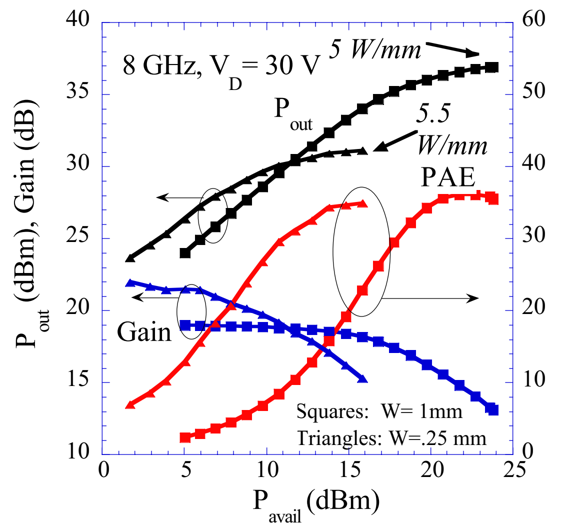

Fig. 3. Comparison of saturated output power, gain, and PAE as a function of input drive power for cascode cells with $W_1 = W_2 =$ 1 mm and μm and $W_1 = W_2 = 0.25$ mm $L_{G1} = L_{G2} = 0.3$ μm under conditions of $V_D = 30$V, $V_{G1} = -3$ V, $V_{G2} = +5$ V, and a frequency of 8 GHz.

A. Broadband Lossy-Match Amplifier

Design: Using two 1 mm cascode cells described in the previous section, a wideband amplifier was created by absorbing the capacitance on the input of the cascode into artificial transmission line sections according to the design

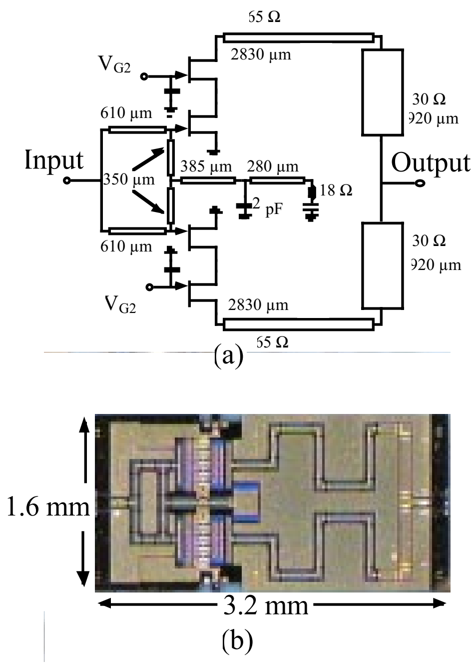

Fig. 4. (a) Circuit diagram and (b) chip photo of lossy-match broadband amplifier. Input matching network transmission lines have impedance $Z_0 = 80\ \Omega$.

technique depicted in Fig. 4 (a). This broadband design technique reduces the device gain at low frequencies and establishes a cutoff frequency approximated by $f_c \approx \frac{1}{\pi\sqrt{LC}}$, where L and C are defined by the cascode device's input capacitance and the additional constraint on the inductance given by $Z_0 = \sqrt{\frac{L}{C}}$. The output matching sections of the amplifier are π-sections, consisting of the shunt output capacitance of the cascode device in series with the series inductance and shunt capacitance provided by a 65 Ω to 30 Ω step in the transmission line impedance. A nonlinear Curtice cubic device model based on parameter extraction of the $0.3 \times 250\ \mu m^2$ device [8] was used for the circuit design and optimization. Using the device model and these design guidelines, the amplifier was designed and fabricated. Figure 4 (b) shows a photograph of the finished amplifier.

Experimental Results: As seen in Fig. 5 (a), on-wafer power measurements using a Focus Microwaves™ load-pull system, with the input and output impedances to the circuit set to 25 Ω and a constant input power of 29 dBm, resulted in an output power of 5-7.5 W over a 3-8 GHz frequency range. As seen from the figure, the achieved PAE's are 20-33 % over this range. Figure 5 (b) shows the saturation characteristics of the power amplifier measured at 6 GHz, where a small signal gain of 15 dB, an output power of 6.3 W and a PAE of 30% were obtained. The bias point of the amplifier for all of these data was $V_D = 25$ V, $V_{G1} = -3$ V, and V_{G2}=5 V. To the authors' knowledge, this is the highest reported output power for a multi-octave bandwidth, solid state, monolithic amplifier.

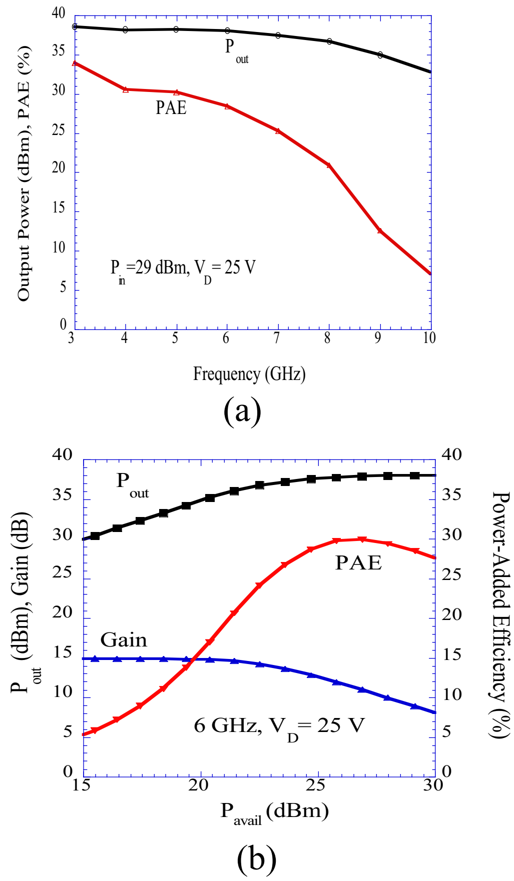

Fig. 5. (a) Saturated output power, Gain, and PAE as a function of frequency for the broadband cascode power amplifier under the conditions of $V_D = 25$ V, $V_{G1} = -3$ V, $V_{G2} = +5$V, $Z_S = Z_L = 25\ \Omega$ and at an input power of 29 dBm. (b) Output power and PAE as a function of input drive power for the broadband cascode power amplifier under the conditions of $V_D = 25$ V, $V_{G1} = -3V$, $V_{G2} = +5V$,$Z_S = Z_L = 25\Omega$, and at a frequency of 6 GHz.

B. *Nonuniform Distributed Amplifier (NDA)*

Design: Three cascode-connected AlGaN/GaN HEMT cells, based on the approach of [4], with $L_{G1} = L_{G2} = 0.3\ \mu$m and $W_{G1} = W_{G2} = 1$ mm, were employed in the design of the NDA. A uniform distributed amplifier, having a drain line termination dummy load, was designed initially to ensure the DC through 8 GHz bandwidth. Then, the drain line termination load was removed, and the gate and drain line sections were optimized to achieve high efficiency operation.

The schematic of the amplifier designed is shown in Fig. 6 (a). The NDA inductances are realized using 80 Ω coplanar waveguides with the lengths indicated in Fig. 6 (a). The gate and drain inductive line lengths were found to optimize the amplifier's gain, bandwidth, and efficiency. The photograph of the fabricated circuit is shown in Fig. 6 (b).

Experimental Results: On-wafer large signal measurements yielded a CW power of 3-6 W over 3-8 GHz and a maximum PAE of 31 % with 6 W of associated output power at 3 GHz. These measurement results, shown in Fig. 7 (a), were taken at $P_{in} = 26$ dBm with source and load impedance set to 25 Ω at each frequency using tuners . The bias conditions for these measurements were

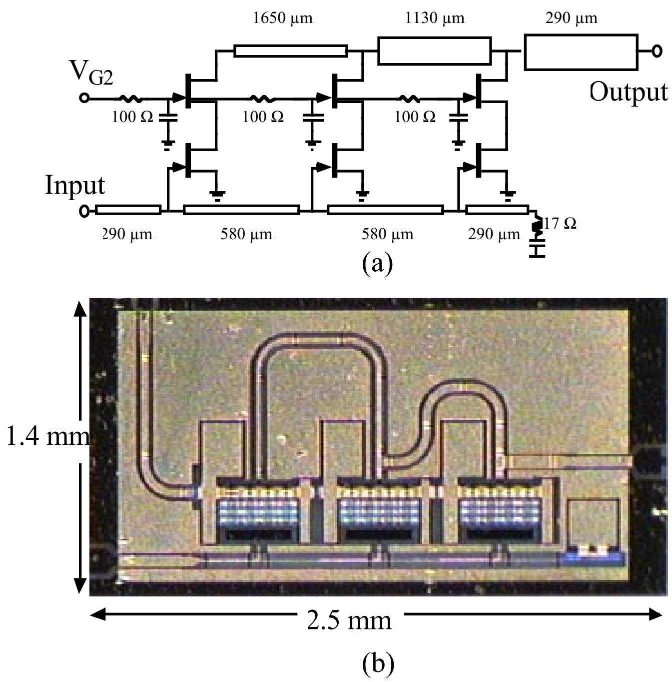

Fig. 6. Fabricated cascode-connected AlGaN/GaN HEMT NDA. (a) Circuit schematic. (b) Circuit photograph. Die size : 2.5 × 1.4 mm^2. All gate CPW line impedances are 80 Ω, and the drain line impedances, from left to right, are 60 Ω, 50 Ω, 30 Ω.

V_D=25 V, V_{G1}=-3 V, and V_{G2}= 5 V (Class A operation). With the same bias condition, the power sweep of Fig. 7 (b) was measured at 5 GHz. As shown in Fig. 7 (b), the fabricated NDA demonstrates broad dynamic range with a small signal gain of over 12 dB. This large signal performance was achieved by means of the high power-gain combination from the broadband MMIC NDA, which is the best reported for a solid-state monolithic distributed amplifier. Using GaAs and cascode circuit technology, a maximum of 2 W (pulsed) has been reported recently for a 2-8 GHz GaAs cascode HBT MMIC DA [10].

IV. Conclusion

An AlGaN/GaN MMIC technology and realization of multi-octave power amplifiers have been presented. The large signal performance of cascode power cells shows the excellent electrical and thermal properties of the devices resulting in high output power and excellent power scaling properties. State-of-the-art multi-octave power performance was obtained using the cascode configuration in both lossy-match and NDA broadband power amplifier designs.

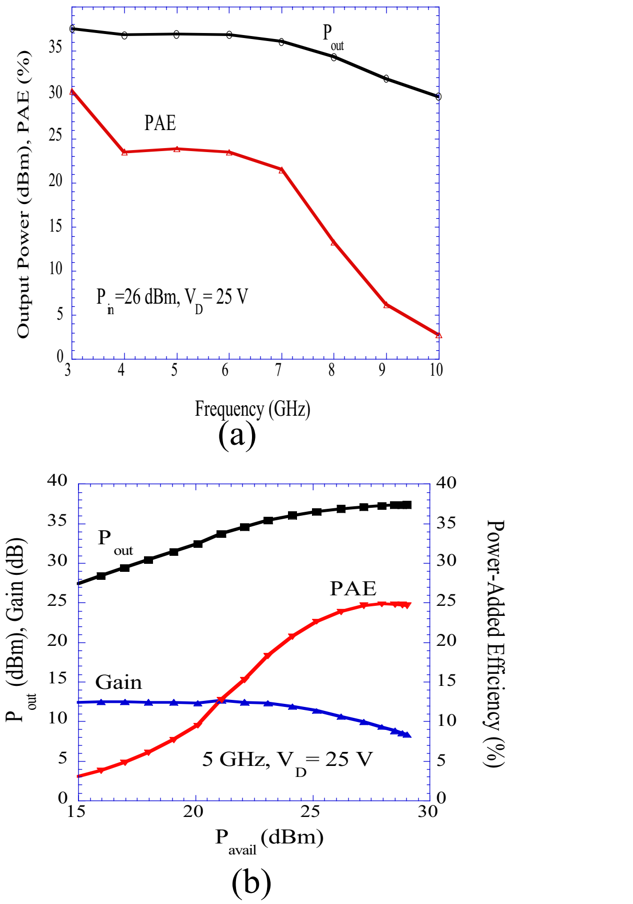

Fig. 7. Measured large signal results for the cascode-connected HEMT NDA with 25 Ω source and load impedances. (a) Power spectrum measured at P_{in} = 26 dBm. (b) Power sweep at 5 GHz.

References

[1] Y.-F. Wu, D. Kapolnek, J. Ibbetson, N.-Q. Zhang, P. Parikh, B.P. Keller, and U.K. Mishra, "High Al-content AlGaN/GaN HEMTs on SiC substrates with very high power performance," in *IEDM Digest*, Washington D.C., Dec. 1999, pp. 925–927.

[2] L.F. Eastman, V. Tilak, B.M. Green, H. Kim, T. Prunty, E.M. Chumbes, J. Smart, R. Dimitrov, and J.R. Shealy, "Polarization induced AlGaN/GaN HEMT's," in *Proc. Cornell Conf. on High Performance Devices*, Ithaca, N.Y., Aug. 2000, pp. 242–246.

[3] J.J. Xu, S. Keller, G. Parish, S. Heikman, U.K. Mishra, and R.A. York, "A 3-10 GHz GaN-based flip-chip integrated broad-band power amplifier," *IEEE Trans. Microwave Theory Tech.*, vol. 48, no. 12, pp. 2573–2578, Dec. 2000.

[4] B.M. Green, K.K. Chu, V. Tilak, J.A. Smart, J.R. Shealy, and L.F. Eastman, "Cascode connected AlGaN/GaN HEMT's on SiC substrates," *IEEE Microwave and Guided Wave Letters*, vol. 10, no. 8, pp. 316–318, August 2000.

[5] B.M. Green, S. Lee, K. Chu, K.J. Webb, and L.F. Eastman, "High Efficiency gallium nitride monolithic distributed amplifer," *IEEE Microwave and Guided Wave Lett.*, vol. 10, no. 7, pp. 270–272, July 2000.

[6] S.T. Sheppard, W.L. Pribble, D.T. Emerson, Z. Ring, R.P. Smith, S.T. Allen, J.W. Milligan, and J.W. Palmour, "AlGaN/GaN HEMT MMIC development," in *Cornell Conf. on High Performance Devices*, Ithaca, N.Y., Aug. 2000, pp. 232–236.

[7] B.M. Green, K.K. Chu, E.M. Chumbes, J.A. Smart, J.R. Shealy, and L.F. Eastman, "The role of surface passivation on the microwave characteristics of AlGaN/GaN HEMTs," *IEEE Electron Device Lett.*, vol. 21, no. 6, pp. 268–270, June 2000.

[8] B.M. Green, K.K. Chu, H. Kim, V. Tilak, J.A. Smart, J.R. Shealy, and L.F. Eastman, "Validation of a large signal model for AlGaN/GaN HEMT's," in *2000 MTT-S Symposium Digest*, Boston, Mass., 2000.

[9] E. L. Ginzton, W. R. Hewlett, J. H. Jasberg, and J. D. Noe, "Distributed amplification," *Proc. IRE*, vol. 36, pp. 956–969, Aug. 1948.

[10] J. Ph. Fraysse, J. P. Viaud, M. Campovecchio, Ph. Auxemery, and R. Quere, "A 2 W, high efficiency, 2-8 GHz, cascode HBT MMIC power distributed amplifier," in *2000 IEEE MTT-S Int. Microwave Symp. Dig.*, Boston, Mass., June 2000, pp. 529–532.